Available online at www.sciencedirect.com
SCIENCE DIRECT
Journal of Catalysis 231 (2005) 1–10
JOURNAL OF CATALYSIS
www.elsevier.com/locate/jcat

Zirconia-supported 12-tungstophosphoric acid as a solid catalyst for the synthesis of linear alkyl benzenes

Biju M. Devassy [a], F. Lefebvre [b], S.B. Halligudi [a,*]

[a] *Inorganic Chemistry and Catalysis Division, National Chemical Laboratory, Pune 411 008, India*
[b] *Laboratoire de Chemie Organometallique de Surface, CNRS-CPE, Villeurbanne cedex, France*

Received 10 July 2004; revised 22 September 2004; accepted 23 September 2004

Available online 28 December 2004

Abstract

The liquid-phase alkylation of benzene with 1-octene and 1-dodecene was investigated with zirconia-supported 12-tungstophosphoric acid (TPA) as catalysts. We prepared the catalysts, with different TPA loading (5–20 wt% calcined at 750 °C) and calcination temperatures (15 wt% calcined from 650 to 850 °C), by suspending hydrous zirconia in a methanol solution of TPA, followed by drying and calcination. These catalysts were characterized by X-ray diffraction, DTG-DTA, FTIR pyridine adsorption, NH_3-TPD, and ^{31}P MAS NMR spectroscopy measurements. The catalyst with optimum TPA loading (15%) and calcination temperature (750 °C) was prepared in different solvents and characterized by ^{31}P MAS NMR spectroscopy. The XRD results indicate that TPA stabilizes the tetragonal phase of zirconia. The catalysts show both Brønsted and Lewis acidity, and 15% TPA on zirconia calcined at 750 °C shows the highest acidity. ^{31}P MAS NMR spectra show two types of phosphorous species: one is the Keggin unit and the other is the decomposition product of TPA. The relative amount of each depends on TPA loading, calcination temperature, and the solvent used for the catalyst preparation. Under reaction conditions of 84 °C and a benzene/1-olefin molar ratio of 10 (time 1 h), the most active catalyst, 15% TPA, calcined at 750 °C, gave more than 98% olefin conversion with selectivity for 2-phenyl octane (53.5%) and 2-phenyl dodecane (47%).

Keywords: Zirconia; 12-Tungstophosphoric acid; Solvent effect; Linear alkyl benzene

1. Introduction

The alkylation of aromatic hydrocarbons with olefins is applied on a large scale in the chemical industry. Alkylation of benzene with $C_{10–14}$ linear alkenes is used for the synthesis of linear alkyl benzenes (LABs), which are the primary raw material for the production of LAB sulfonates, a surfactant detergent intermediate [1]. Traditionally this reaction is catalyzed by a homogeneous Lewis acid such as $AlCl_3$ or a strong Brønsted acid such as HF, which are highly toxic, generate a substantial amount of waste, and cause severe corrosion problems. At present, considerable efforts are being made to find efficient, sustainable, recyclable, and eco-friendly solid acid catalysts that can successfully catalyze the above reaction [2,3]. Various catalysts, such as zeolites, clays, heteropoly acids (HPAs), sulfated zirconia, and immobilized ionic liquids, were tested for this reaction [4–8]. The Detal process developed by UOP uses solid acid catalysts for the alkylation of benzene with heavy olefins under liquid-phase conditions [1].

HPAs are a unique class of materials that are active both in redox and acid catalysis [9,10]. These are polyoxometalates made up of heteropoly anions with metal–oxygen octahedra as the basic structural unit. The Keggin-type HPAs are the most important in catalysis, 12-tungstophosphoric acid (TPA) is the usual catalyst of choice because of its high acidic strength, relatively high thermal stability, and lower oxidation potential compared with molybdenum HPAs. They are strong Brønsted acid catalysts, and their acidity is stronger than that of conventional solid acids like zeolites and mixed oxides.

* Corresponding author.
E-mail address: halligudi@cata.ncl.res.in (S.B. Halligudi).

0021-9517/$ – see front matter
doi:10.1016/j.jcat.2004.09.024

HPAs can be used either directly as a bulk material or in supported form. The supported form is preferable because of its high surface area compared with the bulk material (5–8 $m^2\,g^{-1}$) and better accessibility of reactants to the active sites. Acidic or neutral solids, such as silica, active carbon, and acidic ion-exchange resin, which interact weakly with HPAs, have been reported to be suitable as HPA supports [11]. Serious problems associated with these types of materials are their susceptibility to deactivation during organic reactions due to the formation of carbonaceous deposits (coke) on the catalyst surface. The thermal stability of HPAs is not high enough for conventional regeneration by the burning of coke at 500–550 °C, as routinely used in the case of zeolites and aluminosilicates [12]. Thus the preparation of an active and stable HPA in supported form is essential to utilize fully the potential of these materials as catalysts.

In recent years zirconia has attracted much attention as both a catalyst and a catalyst support because of its high thermal stability and the amphoteric character of its surface hydroxyl groups [13,14]. Extensive studies have been carried out on zirconia modified by isopolytungstate (WO_x–ZrO_2), which acts as an efficient solid acid catalyst [15–17]. But relatively few works are reported on zirconia modified by heteropolytungstates as a catalyst in acid-catalyzed reactions [18–20].

Recently we have shown that zirconia can be used as a suitable support for heteropolytungstate, for example, for 12-TPA [21]. The present study deals with the preparation, characterization, and application of zirconia-supported TPA in the synthesis of LAB by alkylation of benzene with higher linear alkenes such as 1-octene and 1-dodecene. The catalyst with optimum TPA loading and calcination temperature was prepared in different solvents to study the role of the solvent used for catalyst preparation in deciding its catalytic activity in the above reaction. The catalysts were characterized by X-ray diffraction, DTG-DTA, FTIR pyridine adsorption, NH_3-TPD, and ^{31}P MAS NMR spectroscopy.

2. Experimental

2.1. Chemicals

Zirconyl chloride ($ZrOCl_2 \cdot 8H_2O$) and ammonia (25%) were obtained from S.D. Fine Chemicals, Ltd. (Mumbai). 1-Octene (98%), 1-dodecene (95%), 12-TPA ($H_3PW_{12}O_{40} \cdot xH_2O$), and all other solvents (99.9%) were purchased from Aldrich. Benzene (99.7%) was obtained from E. Merck India, Ltd. (Mumbai). All of the chemicals were used as received without further purification.

2.2. Catalyst preparation

We prepared the catalysts by suspending a known amount of dried zirconia powder in a methanol solution of TPA. Zirconium hydroxide was prepared by hydrolysis of 0.5 M zirconyl chloride solution by the dropwise addition of aqueous NH_3 (10 M) to a final pH of 10. The precipitate was filtered and washed with ammoniacal water (pH 8) until it was determined to be free from chloride ions by the silver nitrate test. The hydrous zirconia thus obtained was dried at 120 °C for 12 h, powdered well, and dried for another 12 h. Each time, 4 ml of methanol per gram of solid support was used, and the mixture was stirred in a rotary evaporator for 8–10 h. After stirring, the excess methanol was removed at ca. 50 °C under vacuum. The resulting solid materials were dried at 120 °C for 24 h and ground well. We prepared a series of catalysts with different TPA loading by changing the TPA concentration in methanol. The dried samples were then calcined in air at 750 °C. Samples with 15% TPA were calcined between 650 and 850 °C to understand the role of the calcination temperature on the properties and activity of the catalysts. All samples were calcined in shallow quartz boats placed inside a 3-cm-diameter quartz tube in a tube furnace. The samples were heated at a rate of 5 °C min^{-1} to the final temperature, held for 4 h under static conditions, and cooled at a rate of 5 °C min^{-1} to room temperature. To understand the role of the solvent used for the preparation, the catalyst with optimum TPA loading (15%) was prepared with different solvents. For comparison, we also prepared a catalyst with 15% TPA simply by grinding a mixture of zirconium hydroxide and TPA (neat) for 10 min, followed by drying and calcination as mentioned above. The catalysts are represented by x TZ-t, where x represents weight percentage, T represents TPA, Z represents zirconia, and t denotes calcination temperature (°C).

2.3. Characterization

The specific surface areas of the catalysts were measured by N_2 physisorption at liquid nitrogen temperature with a Quantachrome Nova-1200 surface area analyzer and standard multipoint BET analysis methods. Samples were dried at 300 °C in a dynamic vacuum for 2 h before N_2 physisorption measurements.

X-ray diffraction (XRD) measurements of the catalyst powder were recorded with a Rigaku Geigerflex diffractometer equipped with Ni-filtered Cu-K_α radiation (λ = 1.5418 Å). The volume percentage of the tetragonal phase (V_t) of the calcined samples was estimated with the formula proposed by Toraya et al. [22]:

$$X_m = \frac{I_m(11\text{-}1) + I_m(111)}{I_m(11\text{-}1) + I_m(111) + I_t(111)},$$

$$V_m = \frac{1.311X_m}{1 + 0.31X_m} \quad \text{and} \quad V_t = 1 - V_m,$$

where $I_m(hkl)$ is the integral intensity of the (hkl) reflections of the monoclinic phase and $I_t(111)$ is the intensity of the (111) reflection of the tetragonal phase.

Thermogravimetric and differential thermal analysis (TG-DTA) measurements were performed on a Setaram TG-DTA

92 apparatus from room temperature to 1000 °C in flowing dry air (ca. 50 ml min^{-1}), with α-Al_2O_3 as a reference. For each experiment 25–30 mg of the sample was used, with a heating rate of 10 °C min^{-1}. TGA curves are depicted as first derivative DTG of the direct weight loss traces.

The nature of the acid sites (Brønsted and Lewis) of the catalyst samples was characterized by in situ FTIR spectroscopy with chemisorbed pyridine. For catalysts with different TPA loading, we performed pyridine adsorption (Nicolet model 60 SXB) studies by heating in situ a self-supporting wafer (20 mg) of the sample from room temperature to 400 °C at a rate of 5 °C min^{-1} under vacuum (10^{-6} mbar). The samples were kept at 400 °C for 3 h, followed by cooling to 100 °C. Pyridine vapor (10 mm Hg) was introduced into the cell and allowed to equilibrate for 45 min, followed by evacuation at 100 °C for 30 min, and the IR spectrum was recorded. Then the temperature was slowly increased and IR spectra were recorded at different temperatures up to 400 °C.

The FTIR (Shimadzu SSU 8000) pyridine adsorption studies for the 15 TZ catalyst calcined at different temperatures were carried out in the diffuse reflectance infrared Fourier transform (DRIFT) mode. A calcined powder sample in a sample holder was placed in a specially designed cell. The samples were then heated in situ from room temperature to 400 °C at a rate of 5 °C min^{-1} in a flowing stream (40 ml min^{-1}) of pure N_2. The samples were kept at 400 °C for 3 h and then cooled to 100 °C. Pyridine vapor (20 µl) was then introduced under N_2 flow, and the IR spectra were recorded at different temperatures up to 400 °C. We attained a resolution of 4 cm^{-1} after averaging over 500 scans for all of the IR spectra reported here.

The total amount of acid sites present on the catalysts was evaluated by temperature-programmed desorption (TPD) of NH_3. It was carried out after 0.1 g of the catalyst sample was dehydrated at 500 °C in dry air for 1 h and purged with helium for 0.5 h. The temperature was decreased to 125 °C under a flow of helium, and then 0.5-ml NH_3 pulses were supplied to the samples until no further uptake of ammonia was observed. NH_3 was desorbed in He flow by an increase in the temperature to 540 °C at 10 °C min^{-1}, and NH_3 desorption was measured with a TCD detector.

^{31}P MAS NMR spectra (Bruker DSX-300 spectrometer) were recorded at 121.5 MHz with high power decoupling with a Bruker 4-mm probe head. The spinning rate was 10 kHz, and the delay between two pulses was varied between 1 and 30 s to ensure that complete relaxation of the ^{31}P nuclei occurred. The chemical shifts are given relative to external 85% H_3PO_4.

2.4. Catalyst testing

The liquid-phase alkylation reactions were carried out in a 50-ml glass batch reactor (slurry reactor) with an anhydrous $CaCl_2$ guard tube. The temperature was maintained with a silicon oil bath equipped with a thermostat and a magnetic stirrer; the temperature was measured at the reaction mixture. The catalyst, freshly activated at 500 °C for 2 h, was weighed in the reactor, and then benzene was added according to the desired proportion. Finally, 1-alkene was added to obtain the desired molar ratio of benzene to 1-alkene. For example, a typical reaction mixture consists of 21.86 g (280 mmol) of benzene and 3.14 g of 1-octene (28 mmol), together with 0.125 g of catalyst. After 1 h, the reaction was stopped and the catalyst was separated. The filtrate was analyzed with a Shimadzu 14B gas chromatograph and a HP-5 capillary column (cross-linked 5% ME silicone, 30 m × 0.53 × 1.5 µm film thickness), coupled with FID. Products were identified by GC-MS.

3. Results and discussion

3.1. Characterization of the catalysts

3.1.1. Surface area

The pure zirconium hydroxide dried at 120 °C showed a surface area of 331.6 $m^2\,g^{-1}$. After calcination at 750 °C, the surface area decreased to 16 $m^2\,g^{-1}$. Addition of TPA to the support results in an increase in the surface area, which reaches maximum at ca. 53.2 $m^2\,g^{-1}$ for 15% TPA loading (Table 1). Since this increase is affected by the change in weight of the catalyst by loading, the surface area per gram of the support indicated that the loading of TPA gradually increased the surface area. This can be explained by the fact that the added TPA forms a surface overlayer that reduces the surface diffusion of zirconia and inhibits sintering. It stabilizes the tetragonal phase of zirconia, which leads to an increase in surface area.

The nominal WO_3 loading corresponding to each TPA loading and calcination temperature is determined to calculate the tungsten (W) surface density from the measured surface area. The W surface densities, expressed as the number of W atoms per square nanometer of area (W atoms nm^{-2}), were obtained with the equation

$$\begin{aligned}&\text{Surface density of W}\\&= \{[WO_3 \text{ loading (wt\%)}/100] \times 6.023 \times 10^{23}\}\\&\quad /[231.8 \text{ (formula weight of } WO_3)\\&\quad \times \text{BET surface area } (m^2\,g^{-1}) \times 10^{18}]\end{aligned}$$

and are presented in Table 1. These results show that an increase in TPA loading results in an increase in the surface density of W. The specific surface area of TZ catalyst also depends on the calcination temperature. The surface density of W increased with the calcination temperature because of the concomitant decrease in the ZrO_2 surface area (Table 1).

3.1.2. X-ray diffraction

The XRD pattern of the catalysts with different TPA loading and calcined at 750 °C (Fig. 1) shows that the presence

Table 1
Surface area, phase composition, FTIR pyridine adsorption and NH_3-TPD data of various catalysts

Sample	S_{BET} ($m^2\ g^{-1}$ of sample)	S_{BET} ($m^2\ g^{-1}$ of ZrO_2)	Surface density ($W\ nm^{-2}$)	t-ZrO_2 (vol%)	B/L[a] (I_{1536}/I_{1442})	Acidity[b] ($NH_3\ nm^{-2}$)
Z-750	16.0	16.0	0	5.6	n.e.[c]	n.e.
5 TZ-750	40.2	42.3	3.18	21.9	0.32	3.44
10 TZ-750	46.3	51.5	5.53	75.7	0.64	4.68
15 TZ-750	53.2	62.5	7.23	84.2	1.06	5.21
20 TZ-750	52.3	65.4	9.75	94.6	0.27	2.65
15 TZ-650	105.4	124.0	3.64	95.4	0.59	2.86
15 TZ-700	78.0	91.6	4.93	93.8	0.92	n.e.
15 TZ-750	53.2	62.5	7.23	84.2	1.50	5.21
15 TZ-800	40.7	47.8	9.46	79.3	1.20	n.e.
15 TZ-850	30.4	35.7	12.66	58.9	n.e.	3.86

[a] For catalysts with different TPA loading, pyridine adsorption was carried out under vacuum and for 15% catalyst with different calcination temperature, it was carried out under N_2 flow.
[b] Acidity values obtained from NH_3-TPD.
[c] Not evaluated.

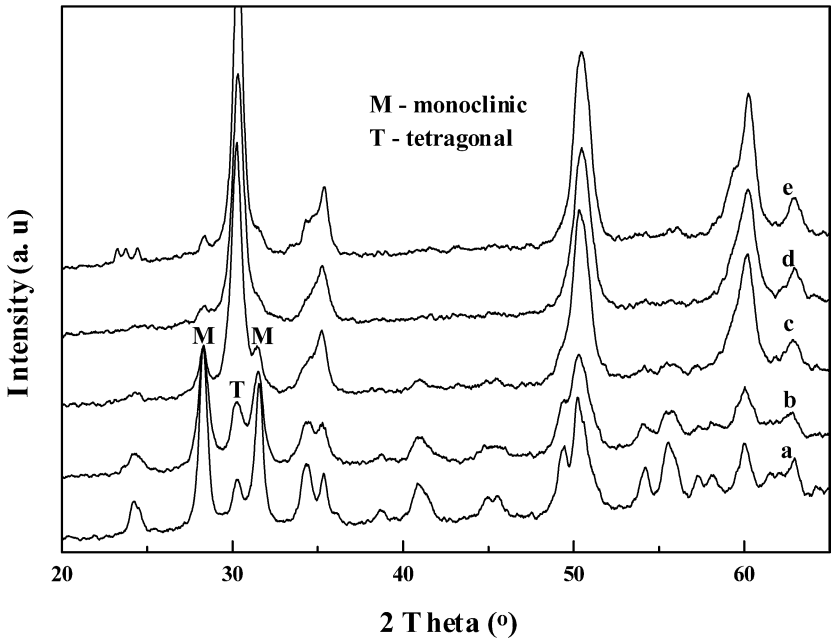

Fig. 1. X-ray diffraction patterns of (a) ZrO_2, (b) 5, (c) 10, (d) 15, and (e) 20% catalysts.

of TPA strongly influences the crystallization of zirconium hydroxide into zirconia. Pure zirconia calcined at 750 °C is mainly monoclinic, with only a small amount of the tetragonal phase (Table 1). For catalysts with low TPA loading and calcined at 750 °C, the XRD pattern can be described as the sum of the monoclinic and tetragonal phases of zirconia; this latter phase becomes dominant for catalyst with 20% TPA. The tetragonal content of zirconia at a fixed loading depends on the calcination temperature; for 15% catalyst, zirconia exists mainly in the tetragonal form at 650 °C, and the tetragonal content decreases with increasing calcination temperature (Table 1).

Thus, the added TPA stabilizes the tetragonal phase of zirconia, and such stabilization of tetragonal ZrO_2 in the presence of TPA and other oxides has been reported in the literature [19,23]. It can also be seen that up to a 15% TPA loading, for catalysts calcined at 750 °C and for 15% catalyst, up to 750 °C calcination, no XRD peaks that could be attributed to the polyacid or to its decomposition products are observed, indicating that TPA is highly dispersed on the support. When the TPA loading is higher than 15%, or when the calcination temperature exceeds 750 °C for 15% loading, new peaks appear in the region of 23–25 °C, which is characteristic of WO_3 [24]. This indicates that (i) TPA decomposes, at least partially, and (ii) tungsten oxide formed by this decomposition is present as relatively large particles. Thus, when the TPA loading exceeds monolayer coverage (see below), the excess TPA that does not interact with zirconia decomposes and the XRD spectra show the presence of bulk crystalline WO_3.

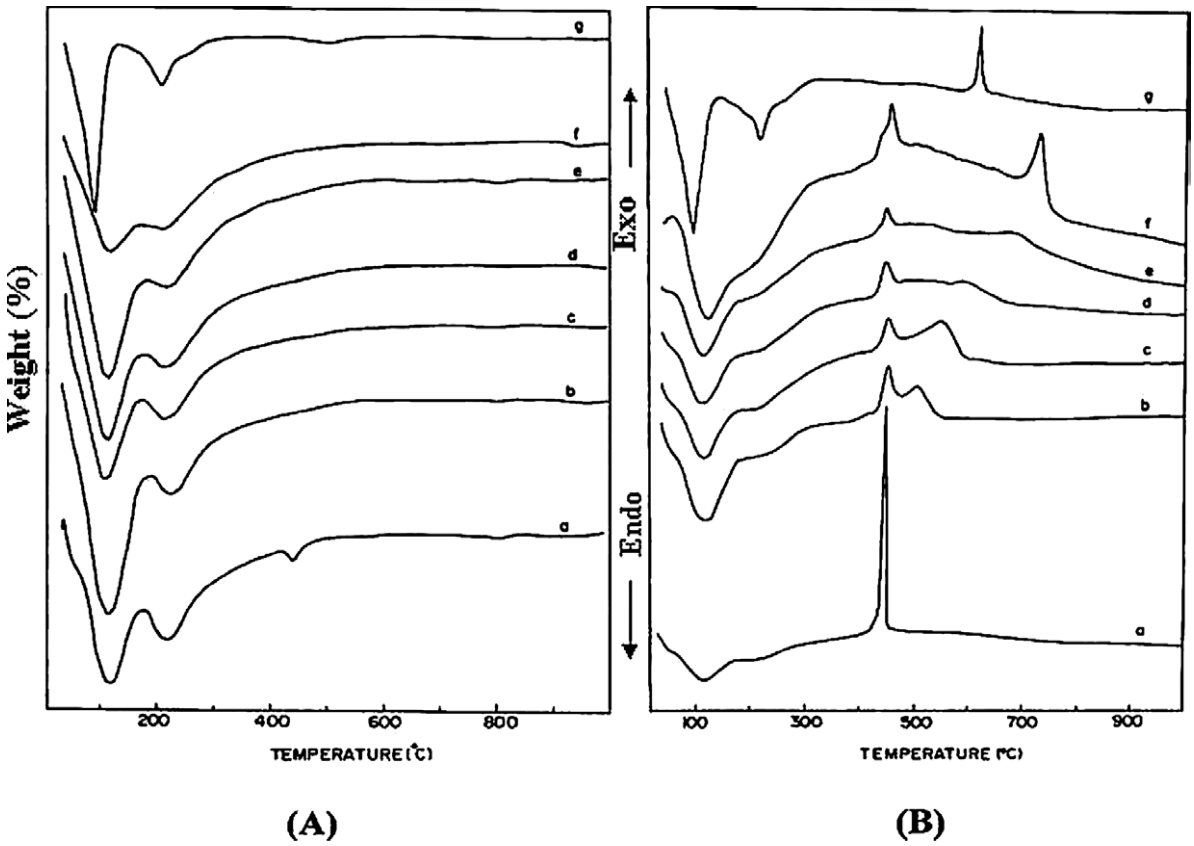

Fig. 2. DTG (A) and DTA (B) curves of (a) hydrous ZrO_2, (b) 5, (c) 10, (d) 15, (e) 20, (f) 30% catalysts, and (g) TPA hydrate.

3.1.3. Thermal analysis (DTG-DTA)

The DTG and DTA spectra of all of the samples dried at 120 °C along with TPA hydrate are shown in Fig. 2. The DTG analysis of pure TPA hydrate ($H_3PW_{12}O_{40} \cdot xH_2O$) shows three stages of weight loss (endothermic effects) [25]. The first weight loss occurred from room temperature to 125 °C because of the loss of physisorbed water. The second one from 130 to 305 °C accounts for the loss of crystallization water, and the third one in the range of 370–550 °C accounts for the loss of 1.5 molecules of H_2O originating from all acidic protons. The total mass loss of the sample corresponded to 21 H_2O molecules per Keggin unit (KU). The DTA shows an exothermic peak at 607 °C due to the complete decomposition of the Keggin structure to form a mixture of oxides followed by its crystallization.

The zirconium hydroxide showed two endothermic and one exothermic peak. The first endothermic peak from room temperature to 180 °C was due to the loss of physisorbed water, and the second peak from 182 to 335 °C was ascribed to the dehydration and dehydroxylation of amorphous zirconium hydroxide. The exothermic effect at 445 °C, termed glow exotherm, is responsible for the crystallization of zirconium hydroxide to metastable tetragonal ZrO_2. The DTG behaviors of all of the TZ samples were almost similar, but differed in DTA behavior. The DTA of the samples shows a broad exothermic peak from 273 to 360 °C with a peak maximum at 305 °C, assigned to the formation of Zr–O–W bonds between TPA's terminal W=O oxygen atoms and surface ≡Zr+ species or to the formation of water by the reaction of TPA protons with ≡ZrOH hydroxyl groups [19,26]. Along with the exothermic effect at 445 °C, another exothermic peak appeared in the temperature range of 500–690 °C for samples with 5–20% TPA, and the peak position moved to higher temperature with increasing TPA content. The sample with 30% TPA showed a sharp exothermic peak at 730 °C. This is due to the crystallization of tungstate species formed by the decomposition of TPA.

3.1.4. FTIR pyridine adsorption

Adsorption of pyridine as a base on the surface of solid acids is one of the most frequently applied methods for the characterization of surface acidity. The use of IR spectroscopy to detect adsorbed pyridine enables us to distinguish among different acid sites. FTIR pyridine adsorption spectra of catalysts with different TPA loading are shown in Fig. 3. The catalysts showed Brønsted (B) and Lewis (L) acidity at 1536 cm^{-1} and at 1442 cm^{-1}; the B/L ratios calculated from the IR absorbance intensities [27] are given in Table 1. The B/L ratio shows that the relative Brønsted acidity increases with TPA loading up to 15% and decreases with further loading. For 15% catalyst, the Brønsted character increases up to 750 °C calcination, and above 750 °C an increase in Lewis acidic character is observed (Table 1). Thus, the catalyst 15 TZ-750 shows the maximum relative

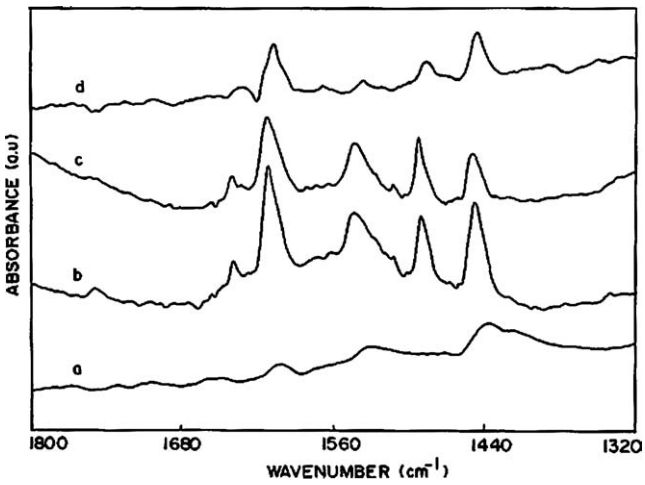

Fig. 3. The IR spectra of pyridine adsorbed on (a) 5, (b) 10, (c) 15, and (d) 20% catalysts after in situ activation at 300 °C.

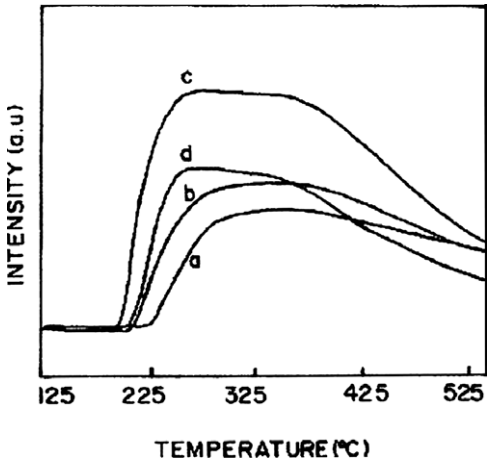

Fig. 4. TPD ammonia profile of (a) 5, (b) 10, (c) 15, and (d) 20% catalysts.

Brønsted acidity, and this corresponds to a monolayer of TPA on ZrO_2.

Since Brønsted acidity increases with calcination temperature up to monolayer coverage, we propose that during calcination, support dehydroxylates and undergoes crystallization, and during this process the interaction of HPA with the support is partially weakened, and some of the H^+ ions that are involved in interaction with the support are freed and act as Brønsted acid sites.

3.1.5. TPD of NH_3

This adsorption–desorption technique permits the determination of the strength of acid sites present on the catalyst surface, together with total acidity. The TPD profiles of the catalysts with different TPA loading are shown in Fig. 4, and the amounts of sorbed NH_3 per square nanometer of the catalysts with different TPA loading and of catalyst with 15% TPA calcined at different temperatures (650, 750, and 850 °C) are given in Table 1. All samples show a broad TPD profile, revealing that the surface acid strength is widely distributed. It is evident from the data that there is an initial increase in the acidity up to 15% loading, and thereafter the acidity decreases. For 15 TZ catalysts, calcined at different temperatures, the amount of adsorbed ammonia increases with calcination temperature and reaches a maximum at 750 °C.

If we take into account the other characterizations, these results can be explained as follows: at lower TPA loadings, the polyoxometalate retains its structure and acidity, whereas for higher loadings it decomposes, at least partially, into its oxides. Thus, the highest acidity corresponds to about one monolayer of polyoxometalate and is evident from ^{31}P MAS NMR spectra. So we can describe the evolution of the catalysts as follows: up to a TPA loading of ca. 15% at 750 °C, or for a 15% catalyst up to a calcination temperature of 750 °C (i.e., up to a monolayer), the heteropolyanion is well dispersed on the zirconia surface and it retains its integrity. When the coverage exceeds a monolayer, the polyanion is not stabilized by zirconia and decomposes to its oxides.

3.1.6. ^{31}P MAS NMR

This is one of the most useful characterization techniques for studying the state of phosphorous in heteropoly acids. The chemical shift depends upon the phosphorous environment and on factors such as hydration number, addenda metal ion, support, etc. [28–32]. The ^{31}P MAS NMR spectra of the catalysts with 5–20% TPA and 15% catalyst calcined from 650 to 850 °C show that the state of phosphorous in the catalyst depends on TPA loading and calcination temperature (Fig. 5). For low loadings and at a calcination temperature of 750 °C, a broad signal above −20 ppm is observed, attributed to phosphorous (P–OH) in the Keggin unit [21,28,32], and at higher loadings and at higher calcination temperatures, a new signal appears below −20 ppm, attributed to phosphorous oxide (P–O–P) resulting from the decomposition of the polyoxometalate [19]. This phosphorous oxide represents 20 and 45% of the total phosphorous for 15 and 20 TZ-750 catalysts and 80% for the 15 TZ-850 catalyst. To the best of our knowledge, this is the highest thermal stability reported so far for any of the heteropoly acid catalysts.

The ^{31}P MAS NMR spectra of catalysts with different TPA loading and calcination temperatures show that the Keggin unit starts decomposition at a TPA loading of ca. 15% at 750 °C. The results from different characterization techniques suggest that a geometric monolayer of TPA on zirconia was attained for 15 TZ-750 catalyst.

The 15 TZ-750 catalyst was selected to study the role of the solvent used for catalyst preparation. The NMR spectra of the catalysts prepared in different solvents show two signals, one above −20 ppm and one below −20 ppm (not shown). A careful examination of the spectra shows that the signal intensities depend upon the solvent used for the catalyst preparation, confirming the vital role played by the solvent in stabilizing the Keggin structure of HPA in the final catalyst. We have observed a direct relation between P–OH

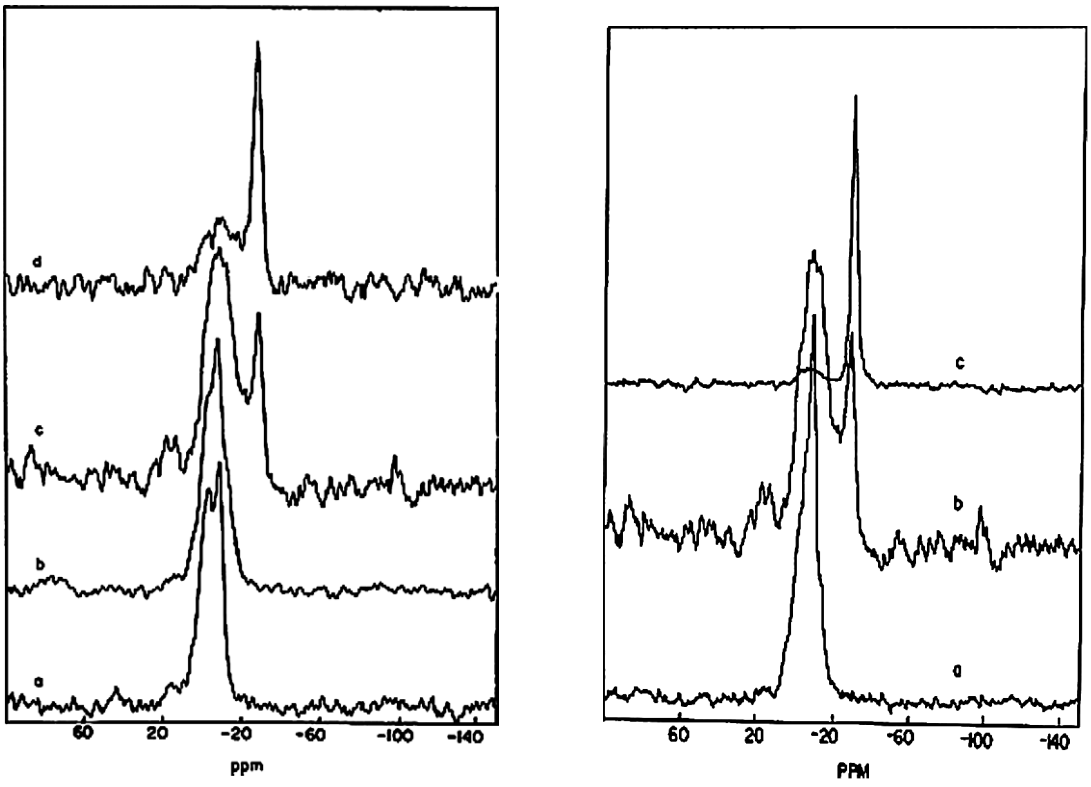

Fig. 5. ^{31}P MAS NMR spectra of (A) catalysts with different TPA loading (a) 5, (b) 10, (c) 15, and (d) 20% and (B) 15% catalyst calcined at different temperature (a) 650, (b) 750, and (d) 850 °C.

Table 2
P–OH intensity, dielectric constant, octene conversion and product selectivity of 15% catalyst prepared in different solvents (conditions: total weight = 25 g; catalyst weight = 0.125 g; temperature = 84 °C; benzene/1-octene (molar ratio) = 10; time = 1 h)

Solvent	Dielectric constant	P–OH[a] intensity (%)	Octene conversion (mol%)	MOB selectivity (%)	DOB selectivity (%)
Neat	–	32	12.1	100	0
Ether	2.21	33	14.2	100	0
1,4-Dioxane	4.30	36	14.3	100	0
Acetic acid	6.20	40	24.0	99.6	0.4
Ethyl acetate	6.02	44	27.0	99.4	0.6
THF	7.60	46	27.6	99.2	0.8
Acetone	20.60	52	32.8	99.4	0.6
Water	79.70	65	43.4	99.0	1.0
Methanol	32.60	80	53.4	95.5	4.5
DMF	36.70	82	55.5	95.4	4.6

[a] Relative amount of TPA in Keggin form.

intensity and the dielectric constant of the solvent [33] used for the catalyst preparation (Table 2). It is evident from Table 2 that the P–OH intensity (i.e., the amount of TPA in Keggin form) increases with the dielectric constant of the solvent, except for water as the solvent.

From spectroscopic studies Rocchiccioli-Deltcheff et al. showed the existence of anion–anion interaction in the acid form of HPA in solid state and in solution [34,35]. The present work shows that the interaction of HPA with solvents varies with the dielectric constant of the solvent. In solvents with a high dielectric constant (e.g., solvents like DMF and methanol), the anion–anion interaction seems to be absent or negligible and the catalyst prepared with such solvents retains a maximum amount of TPA in Keggin form, that is, such catalysts show the highest P–OH intensity. In the case of DMF as a solvent, DMF is protonated by TPA and the protonated DMF interacts with the Keggin anion, as in the case of tetraalkylammonium salts of HPA, explaining the lack of anion–anion interaction for the acid form in DMF [35,36]. TPA in CH_3OH forms protonated monomers ($(CH_3OH_2)^+$) and dimers ($((CH_3OH)_2H^+$), and these ions interact more with Keggin ions than TPA does directly with the solvent [37]. TPA in other solvents under study shows varying degrees of anion–anion interactions arising from the formation of hydrogen-bonding networks in the solvent, resulting in a solvent structure that holds the anion within interaction proximity [35]. Hence we presume that, as the dielectric constant of the solvent decreases, the ability of the solvent to undergo structured solvent and anion–anion interaction increases.

The hydroxyl group of the zirconium hydroxide tends to be either positively or negatively charged below or above the IEP (pH 6–7) [38]. Above the IEP, the hydroxyl groups tend to be negatively charged, so that it is relatively difficult for the anions to be adsorbed on the hydroxide surface, because of electrostatic repulsion. On the other hand, the adsorption

of the anions is favored below the IEP of the support. Hence, the adsorption of tungstophosphate ions on the surface of zirconium hydroxide is favorable when water is used as the solvent, which is not applicable in the case of nonaqueous solvents. The solvent water has the highest dielectric constant (79.7), but the catalyst prepared in water shows a P–OH intensity lower than that prepared in methanol. Here one must consider the stability of TPA in water. The maximum limit for the stability of TPA in water is 0.1 M [35]. However, the concentration of TPA in our experimental condition corresponds to ~ 0.01 M. Thus the low P–OH intensity of the catalyst prepared in water is attributed to the low stability of TPA in water at low concentration.

The different behavior of the catalyst prepared in different solvents can also originate from limitation of diffusion of TPA into the pores of the support. The size of the Keggin anion (12 Å) is on the order of the pore size of the support (diameter < 2 nm) [39]; the rate of diffusion is controlled by the anion size, and the large polyoxoanions should have a lower diffusion rate. Since the HPA anions are very weakly solvated in solvents, the solubility of heteropoly acids depends on the solvation of cations [40]. Thus the effective size of the Keggin unit can vary from solvent to solvent, and hence the diffusivity of the polyanion ultimately results in different dispersion of HPA on the support and hence the amount of intact TPA present in the ZrO_2 surface after calcination. These results are in good agreement with the observations of Fournier et al., who suggest the use of DMF as a solvent to achieve good dispersion during the preparation of supported heteropoly acid catalysts [35]. We have used methanol as a solvent because of its higher volatility and ease in handling.

3.2. Catalytic activity

3.2.1. Alkylation of benzene

With these catalysts, the main reactions were alkene double-bond shift isomerization and benzene alkylation. Monoalkylbenzenes (MOBs) were the main reaction product, whereas dialkylbenzenes (DOBs) and alkene dimers (DIMs) appeared in small amounts. The conversion was expressed as the percentage of alkene converted into products. The effect of TPA loading on octene conversion and product selectivity is shown in Table 3. The 5 TZ catalyst showed 1.3% conversion, and conversion increased to a maximum of 53.4% at 15% loading. The selectivity for mono- and dialkylated products depended on TPA loading, and the catalyst with 15% TPA showed 95.5% monoalkylation selectivity.

To study the effect of calcination temperature, we used 15 TZ catalyst calcined between 650 and 850 °C. The catalyst calcined at 650 °C showed 8.7% octene conversion, and conversion increased to 53.4% at a calcination temperature of 750 °C (Table 3). With an increase in calcination temperature, selectivity for dialkylation increased up to 750 °C and then decreased. The high activity of 15 TZ-750 catalyst is due to its high Brønsted acidity.

Table 3
Octene conversion and product selectivity over various catalysts (conditions: total weight = 25 g; catalyst weight = 0.125 g; temperature = 84 °C; benzene/1-octene (molar ratio) = 10; time = 1 h)

Sample	Octene conversion (mol%)	TOF (10^{-3} mol mol_W^{-1} s^{-1})	MOB selectivity (%)	DOB selectivity (%)
5 TZ-750	1.3	3.7	100	0
10 TZ-750	14.9	20.8	100	0
15 TZ-750	53.4	50.0	95.5	4.5
20 TZ-750	47.6	33.6	97.9	2.1
25 TZ-750	41.1	23.1	98.7	1.3
15 TZ-650	8.7	8.1	100	0
15 TZ-700	34.6	32.5	97.8	2.2
15 TZ-800	24.0	22.5	99.0	1.0
15 TZ-850	5.4	5.0	100	0

To establish the relation between catalytic activity, TPA loading, and calcination temperature, the turnover frequencies (TOF, (mol mol_W^{-1} s^{-1}) of different catalysts were calculated (Table 3). The catalyst 15 TZ-750 showed the highest TOF, and the surface density of this catalyst is found to be 7.23 W nm^{-2} (Table 1), which corresponds to monolayer coverage of TPA on zirconia [21]. This clearly indicates that, irrespective of loading and calcination temperature, catalytic activity depends on TPA coverage, and the highest activity corresponds to monolayer of TPA on zirconia.

Therefore, the catalyst with optimum TPA loading (15%) and calcination temperature (750 °C) was taken to study the role of the solvent used for catalyst preparation. The variation of conversion and selectivity for the 15% catalyst prepared in different solvents showed that the conversion increases with P–OH intensity (Table 2). The catalyst prepared without solvent showed the lowest octene conversion of 12.1%, and the catalyst prepared in DMF showed the highest conversion of 55.5%. As the conversion increased, the selectivity for monoalkylation decreased from 100% for the catalyst prepared without solvent to 95.4% for the one prepared in DMF. It has to be noted that there is not much difference in octene conversion for the catalysts prepared in methanol and DMF.

The 15 TZ-750 catalyst prepared with methanol as a solvent was used to study the effect of temperature in the range of 55–84 °C. The results indicate that temperature has a drastic effect on the conversion of octene (Fig. 6). At 55 °C, the conversion was only 0.4%, and it increased to 6.2% at 75 °C. An increase of 47% octene conversion was observed when the temperature was increased from 75 to 84 °C (boiling point of the reaction mixture).

We studied the effect of the benzene/octene molar ratio (4 to 10) on conversion and product selectivity while keeping the total weight of the reaction mixture constant under otherwise similar conditions (Fig. 6). As the molar ratio was increased from 4 to 10, the octene conversion increased from 29 to 53.4%, and the selectivity for dialkylation decreased from 13.4 to 4.5%. The dimerization of octene was also observed at low benzene/octene molar ratios, and the dimer

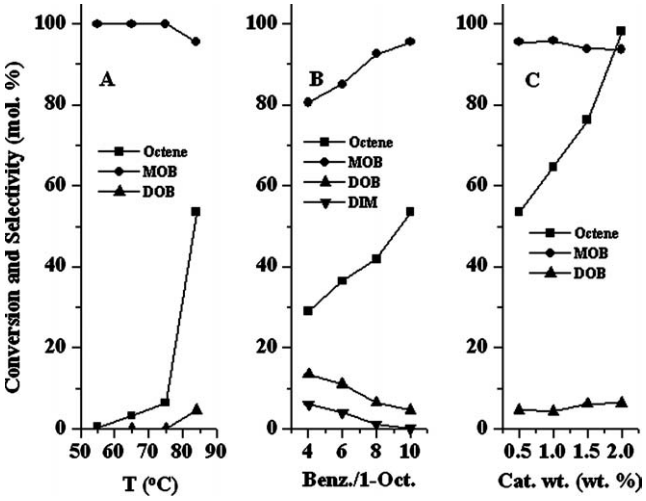

Fig. 6. Effect of reaction conditions on octene conversion and product selectivity. (A) Effect of temperature (conditions: total weight = 25 g; catalyst weight = 0.125 g; benzene/1-octene (molar ratio) = 10; time = 1 h). (B) Effect of molar ratio (conditions: total weight = 25 g; catalyst weight = 0.125 g; temperature = 84 °C; time = 1 h). (C) Effect of catalyst weight (conditions: total weight = 25 g; temperature = 84 °C; benzene/1-octene (molar ratio) = 10; time = 1 h).

content decreased with increasing amount of benzene; it is absent at a molar ratio of 10.

The effect of catalyst concentration on octene conversion shows that a catalyst concentration of 0.5 wt% (of the total mass of the reactants) gave an octene conversion of 53.4%, which increased to 98.1% with 2 wt% catalyst, while the MOB selectivity remained almost the same (Fig. 6). Thus, under reaction conditions of 84 °C, 1 h, and a benzene/olefin molar ratio of 10, alkylation of benzene with 1-octene gave 98.1% octene conversion with 93.7% MOB selectivity (isomer distribution 57.2% 2-PO, 26% 3-PO, and 16.8% 4-PO) and 6.3% DOB selectivity.

Under the above reaction conditions (84 °C, 1 h, and benzene/olefin molar ratio of 10), the reaction of benzene with 1-dodecene was also performed. as the desired product monododecyl benzene (phenyl dodecane—PD) is the precursor to linear alkyl benzene sulfonate, which is the most widely used surfactant in the detergent industry. The 2 wt% catalyst concentration gave a dodecene conversion of 41%, and the conversion increases to 99% with 5% catalyst. As the conversion increased from 41 to 99%, the monododecyl benzene (MDB) selectivity decreased from 98.8 to 95.3%, and didodecyl benzene selectivity increased from 1.2 to 4.7%. At a dodecene conversion of 99%, the MDB isomer distribution was 49.4% 2-PD, 17.3% 3-PD, 11% 4-PD, and 22.3% 5 + 6 PD. Sulfated zirconia was shown to be more active [7], and zeolites are more selective catalysts for 2-isomer, but at low activity for this reaction [41].

For supported heteropoly acid catalysts, it is important to study recycling of the catalyst, since the limited thermal stability of heteropoly acids usually prevents regeneration of the deactivated catalyst by thermal methods. The recyclability of 15 TZ-750 catalyst was tested in the alkylation of benzene with 1-octene at 84 °C (2 wt% catalyst, 1 h, and 10:1 molar reactants ratio). To study the recycling, after the first cycle the catalyst was separated (without washing), dried in air at 80 °C for 4 h, and reused with fresh reaction mixture. After the first use, the catalyst retains only 30% of initial conversion. Thermal analysis of the separated catalyst shows a continuous weight loss (3.8%) in the temperature range of 230–580 °C, attributed to adsorbed products and alkene oligomers. This result suggests that the loss in catalytic activity is due the blockage of active sites of the catalyst by heavy aromatics and oligomerized octene [7]. The deactivated catalyst can be partially regenerated by refluxing with dichloromethane. The dried catalyst obtained after refluxing with dichloromethane gave 60% of initial conversion. After the first recycling, the catalyst was reused twice without appreciable loss in activity, after regeneration. The regeneration was achieved by catalyst separation followed by drying at 120 °C for 4 h and calcination at 600 °C for 4 h in the presence of air. After the second regeneration, the catalyst shows more than 96% initial conversion.

4. Conclusions

Zirconia-supported 12-tungstophosphoric acid acts as an efficient and stable solid acid catalyst. The activity of the catalyst in the alkylation of benzene with 1-octene is found to depend on TPA loading, calcination temperature, and solvent used for the catalyst preparation. Solvents like methanol and DMF are the best for catalyst preparation. The catalyst with a monolayer of TPA on zirconia (15 TZ-750) prepared in methanol showed the highest activity. Under the reaction conditions of 84 °C and a benzene/1-olefin molar ratio of 10 (time 1 h), 15 TZ-750 catalyst gave more than 98% olefin conversion, 53.5% selectivity for 2-phenyl octane, and 47% selectivity for 2-phenyl dodecane.

Acknowledgments

The authors thank the reviewer for constructive suggestions on an earlier version of this paper. This work was carried under a DST-SERC-sponsored project. B.M.D. acknowledges CSIR New Delhi for a research fellowship.

References

[1] J.A. Kocal, B.V. Vora, T. Imai, Appl. Catal. A 221 (2001) 295.
[2] A. Corma, Chem. Rev. 95 (1995) 559.
[3] A. Corma, H. Garcia, Chem. Rev. 103 (2003) 4307.
[4] S. Sivasankar, A. Thangaraj, J. Catal.138 (1992) 386.
[5] J.L.B. Tejero, A.M. Danvila, US Patent 5 146 026 (1992) to Petroquimica Espanola, S.A. Petresa.
[6] R.T. Sebulsky, A.M. Henke, Ind. Eng. Chem. Process Res. Dev. 10 (1971) 272.
[7] J.H. Clark, G.L. Monks, D.J. Nightingale, P.M. Price, J.F. White, J. Catal. 193 (2000) 348.

[8] C. DeCastro, E. Sauvage, M.H. Valkenberg, W.F. Hölderich, J. Catal. 196 (2000) 86.
[9] C.L. Hill (Ed.), Chem. Rev. 98 (1998) 1.
[10] T. Okuhara, N. Mizuno, M. Misono, Adv. Catal. 41 (1996) 113.
[11] S. Damyanova, L.M. Gomez, M.A. Banares, J.L.G. Fierro, Chem. Mater. 12 (2000) 501.
[12] I.V. Kozhevnikov, Chem. Rev. 98 (1998) 171.
[13] K. Tanabe, T. Yamaguchi, Catal. Today 20 (1994) 185.
[14] G.K. Chuah, Catal. Today 49 (1999) 131.
[15] D.G. Barton, S.L. Soled, E. Iglesia, Topics Catal. 6 (1998) 87.
[16] S. Kuba, P. Lukinskas, R.K. Grasselli, B.C. Gates, H. Knözinger, J. Catal. 216 (2003) 353.
[17] F.D. Gregorio, V. Keller, J. Catal. 225 (2004) 45.
[18] E. Lopez-Salinas, J.G. Hermandez-Cortez, M.A. Cortes-Jacome, J. Navarrete, M.E. Llanos, A. Vazquez, H. Armendariz, T. Lopez, Appl. Catal. A 175 (1998) 43.
[19] E. Lopez-Salinas, J.G. Hermandez-Cortez, I. Schifter, E. Torres-Garcia, J. Navarrete, A. Gutierrez-Carrillo, T. Lopez, P.P. Lottici, D. Bersani, Appl. Catal. A 193 (2000) 215.
[20] S. Patel, N. Purohit, A. Patel, J. Mol. Catal. A 192 (2003) 195.
[21] B.M. Devassy, S.B. Halligudi, S.G. Hegde, A.B. Halgeri, F. Lefebvre, Chem. Commun. (2002) 1074.
[22] H. Toraya, M. Yoshimura, S. Somiya, J. Am. Ceram. Soc. C 67 (1984) 119.
[23] A. Khodakov, J. Yang, S. Su, E. Iglesia, J. Catal. 177 (1998) 343.
[24] JCPDS-International Center for diffraction data, 1990, Card 43-1035.
[25] I.V. Kozhevnikov, Catalysts for Fine Chenical Synthesis, Catalysis by polyoxometalates, vol. 2, Wiley, New York, 2002, p. 15.
[26] J.B. Moffat, Catalysis by Acids and Bases, Elsevier, Amsterdam, 1985, p. 157.
[27] B.H. Davis, R.A. Keogh, S. Alerasool, D.J. Zalewski, D.E. Day, P.K. Doolin, J. Catal. 183 (1999) 45.
[28] M. Misono, Chem. Commun. (2001) 1141.
[29] C.J. Dillon, J.H. Holles, R.J. Davis, J.A. Labinger, M.E. Davis, J. Catal. 218 (2003) 54.
[30] A. Ghanbari-Siahkali, A. Philippou, J. Dwyer, M.W. Anderson, Appl. Catal. A 192 (2000) 57.
[31] A. Molnar, T. Beregszaszi, A. Fudala, P. Lentz, J.B. Nagy, Z. Konya, I. Kiricsi, J. Catal. 202 (2001) 379.
[32] S. Uchida, K. Inumaru, M. Misono, J. Phys. Chem. B 104 (2000) 8108.
[33] I.M. Smallwood, Handbook of Organic Solvent Properties, Arnold, London NW1 3BH, 1996.
[34] C. Rocchiccioli-Deltcheff, M. Fournier, R. Franck, R. Thouvenot, Inorg. Chem. 22 (1983) 207.
[35] M. Fournier, R. Thouvenot, C. Rocchiccioli-Deltcheff, J. Chem. Soc. Faraday Trans. 87 (1991) 349.
[36] G. Zukowska, J.R. Stevens, K.R. Jeffrey, Electrochem. Acta 48 (2003) 2157.
[37] Y. Hirano, K. Inumaru, T. Okuhara, M. Misono, Chem. Lett. (1996) 1111.
[38] A.A. Parks, Chem. Rev. 65 (1965) 177.
[39] M. Valigi, D. Gazzoli, G. Ferraris, E. Bemporad, Phys. Chem. Chem. Phys. 5 (2003) 4974.
[40] L.C.W. Baker, D. Glick, Chem. Rev. 98 (1998) 3.
[41] J.L.G. de Almeida, M. Dufaux, Y. Ben Tarrit, C. Naccache, J. Am. Oil Chem. Soc. 71 (7) (1994) 675.